EDM実験

川崎真介

KEK

Electric Dipole Moment (EDM)

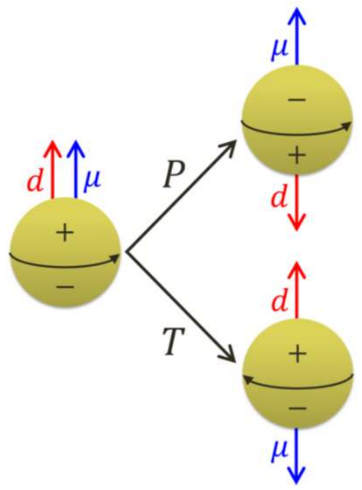

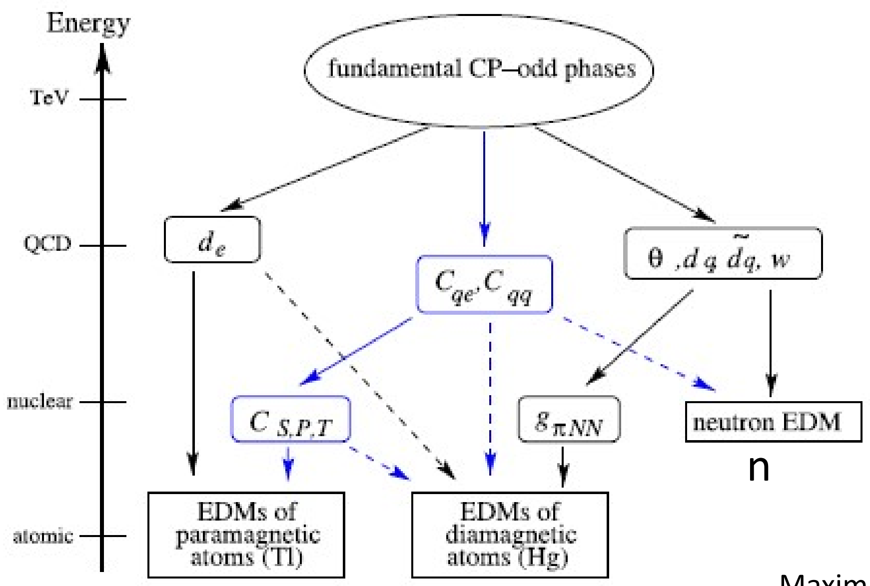

Tl, Fr, Cs.... ^{199}Hg, ^{129}Xe, Rn, Ra...

- Electric dipole moment (EDM)
  - Vector derived from charge distribution

$$\vec{d} = d\,\frac{\vec{s}}{|\vec{s}|}$$

unit   e cm

	P	T
spin	Even	Odd
EDM	Odd	Even

d≠0   → T Violation

Assume CPT conservation

→ CP Violation

new source of CP violation?

EDM search in various kind of system is important to understand nature of physics

Maxim Pospelov and Adam Ritz,
Annals of Physics 318 (2005) 119–169

EDMの大きさ

- 例えば中性子EDMの場合

$$|d_{\mathrm{n}}| < 1.8 \times 10^{-26}\ \mathrm{ecm}$$

Phys. Rev. Lett 124,081803 (2020)

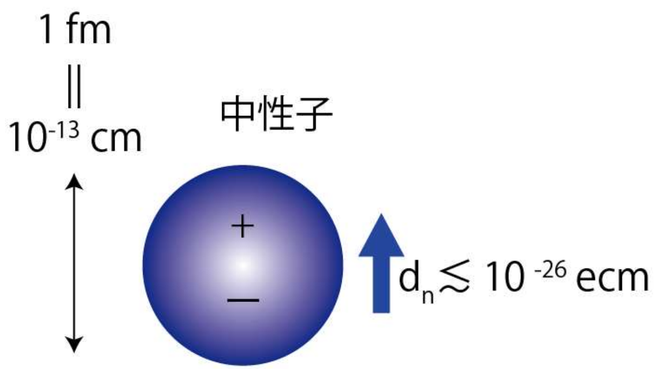

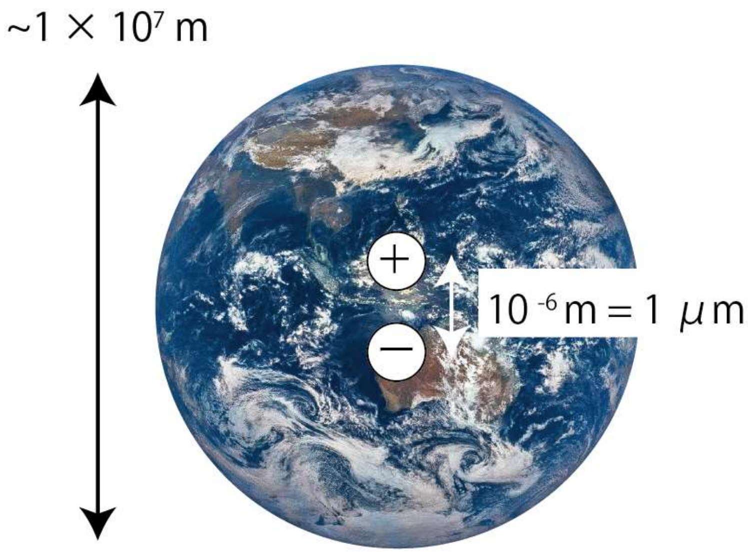

地球の大きさの中から1μm離れた素電荷のを見つけるのと同じスケール感

EDMの測定方法

$$H = -\vec{\mu}\cdot\vec{B} + \vec{d}\cdot\vec{E}$$

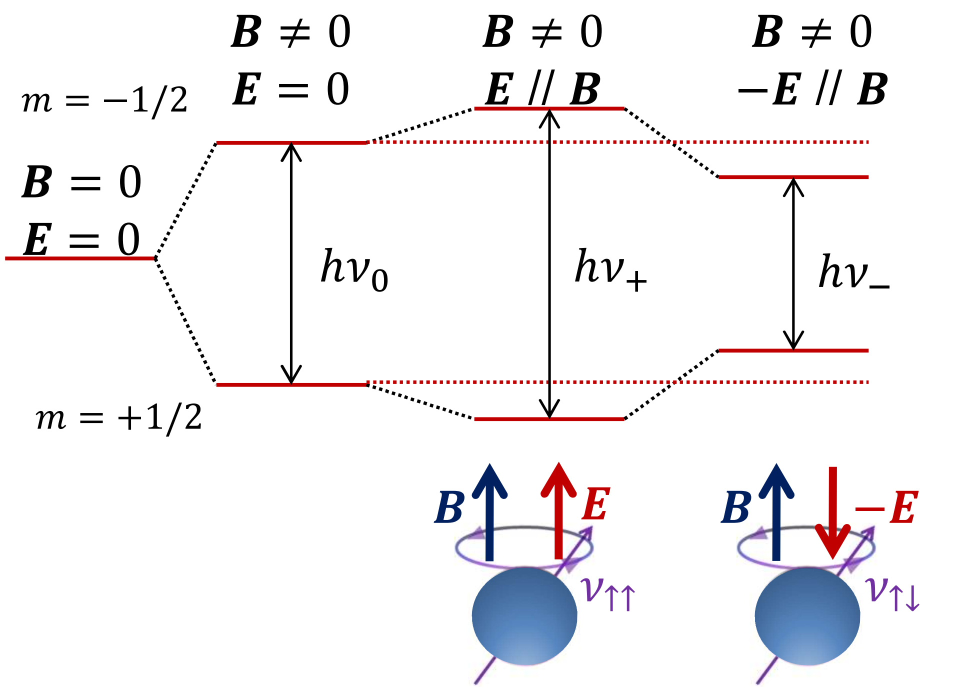

$$\nu_{\uparrow\uparrow} = \frac{2\mu B + 2dE}{h} \qquad \nu_{\uparrow\downarrow} = \frac{2\mu B - 2dE}{h}$$

figure from K. Asahi

(理想的)
電磁場中のスピン歳差運動周期の差を測定

$$\Delta\nu = \nu_{\uparrow\uparrow} - \nu_{\uparrow\downarrow} = \frac{4dE}{h}$$

d = 10^{-26} ecm, E = 10 kVの時

$\Delta\nu$＝1 μHz

Cf. 中性子のラーモア周波数(ν_0)
30 Hz/μT

実際は

$$\Delta\nu = \nu_{\uparrow\uparrow} - \nu_{\uparrow\downarrow} = \frac{2\mu(\boxed{\mathrm{B}_{\uparrow\uparrow} - \mathrm{B}_{\uparrow\downarrow}})}{h} + \frac{4d\boxed{E}}{h}$$

この項が消え切らない

Bの精密制御

E = 10 kVでd = 10^{-26} ecmを測定する場合

$$\Delta B = (\mathrm{B}_{\uparrow\uparrow} - \mathrm{B}_{\uparrow\downarrow}) \ll \frac{dE}{\mu} \sim 10\ \mathrm{fT}$$

磁場を精密に制御するために
- 磁気シールド
- 磁束計
  - SQUID, Cs, Rb
  - Co-magnetometer (^{199}Hg, ^{3}He)

の開発が重要

大きなE

・高電場
・分子、結晶内の有効磁場

History of EDM search

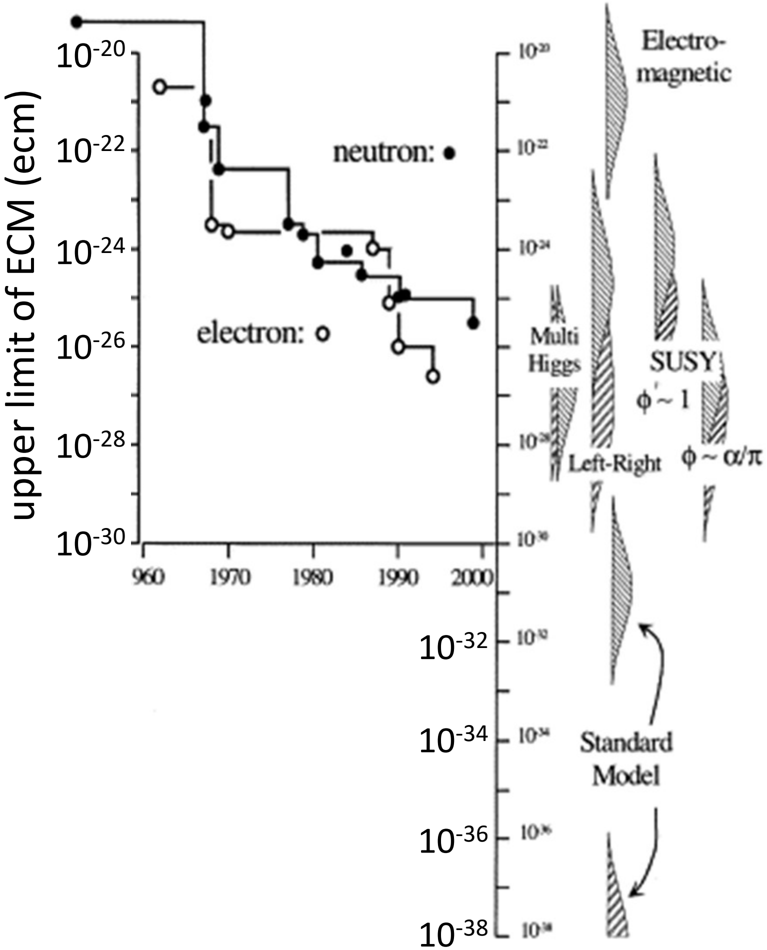

Pendlebury and Hinds, NIM A 440 (00) 471

upper limit

neutron EDM

$|d_n| < 1.8 \times 10^{-26}$ ecm UCN — C. Abel et al. Phys. Rev. Lett. 124, 081803 (2020)

electron EDM

$|d_e| < 1.6 \times 10^{-27}$ ecm Cs

$|d_e| < 1.6 \times 10^{-27}$ ecm Tl — B.C. Regan et al, PRL 88, 071805 (2002)

$|d_e| < 10.5 \times 10^{-28}$ ecm YbF — J. J. Hudson et al, Nature 473, 493 (2011)

$|d_e| < 8.7 \times 10^{-29}$ ecm ThO — The ACME Collaboration et al, Science, 343, 269 (2014)

atomic EDM

$|d_{Hg}| < 7.4 \times 10^{-30}$ ecm ^{199}Hg — B. Garner et al., PRL 116 161601 (2016)

$|d_{Xe}| < 1.5 \times 10^{-27}$ ecm ^{129}Xe — F. Allmendinger et al, Phys. Rev. A 100, 022505 (2019)

muon EDM

$|d_{\mu}| < 1.8 \times 10^{-19}$ ecm — G. W. Bennett et al, Phys. Rev. D 80, 052008 (2009)

Standard model prediction

neutron : 10^{-30} – 10^{-32} ecm

electron : 10^{-37} – 10-^{40} ecm

much smaller than current experimental sensitivity

good probe of testing new physics

中性子EDM

Ultra Cold Neutron (UCN)

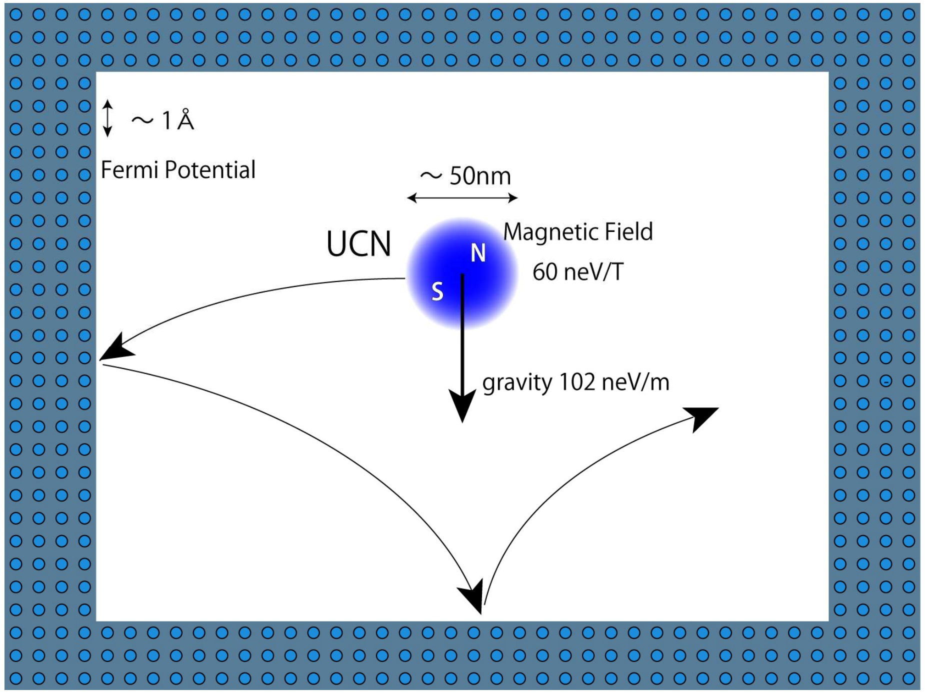

Ultra Cold Neutron

Energy	~ 100 neV
Velocity	~ 5 m/s
Wave length	~ 50 nm

Interaction

- Gravity 100 neV/m
- Magnetic field 60 neV/T
- Weak interaction
  - β-decay n → p + e
- Strong interaction
  - Fermi potential 335 neV (^{58}Ni)
    - atom distance : ~ Å
    - UCN feels average nuclear potential

Unique property

UCN can be confined in material bottle

→ Use various experiments

nEDM, n lifetime, gravity ....

UCN Source at ILL
UCN turbine

Institute Laue-Langevin
Grenoble, France
Reactor 57MW

UCN Production		
reactor neutron	~100 meV	
Liq. D_2 25K	~1 meV	
vertical guide	~100 μeV	→ VCN
Turbine	~100 neV	→ UCN

Turbine UCN source

slow down by reflection on the moving mirror

Restriction by Liouville's theorem

conservation of phase space density

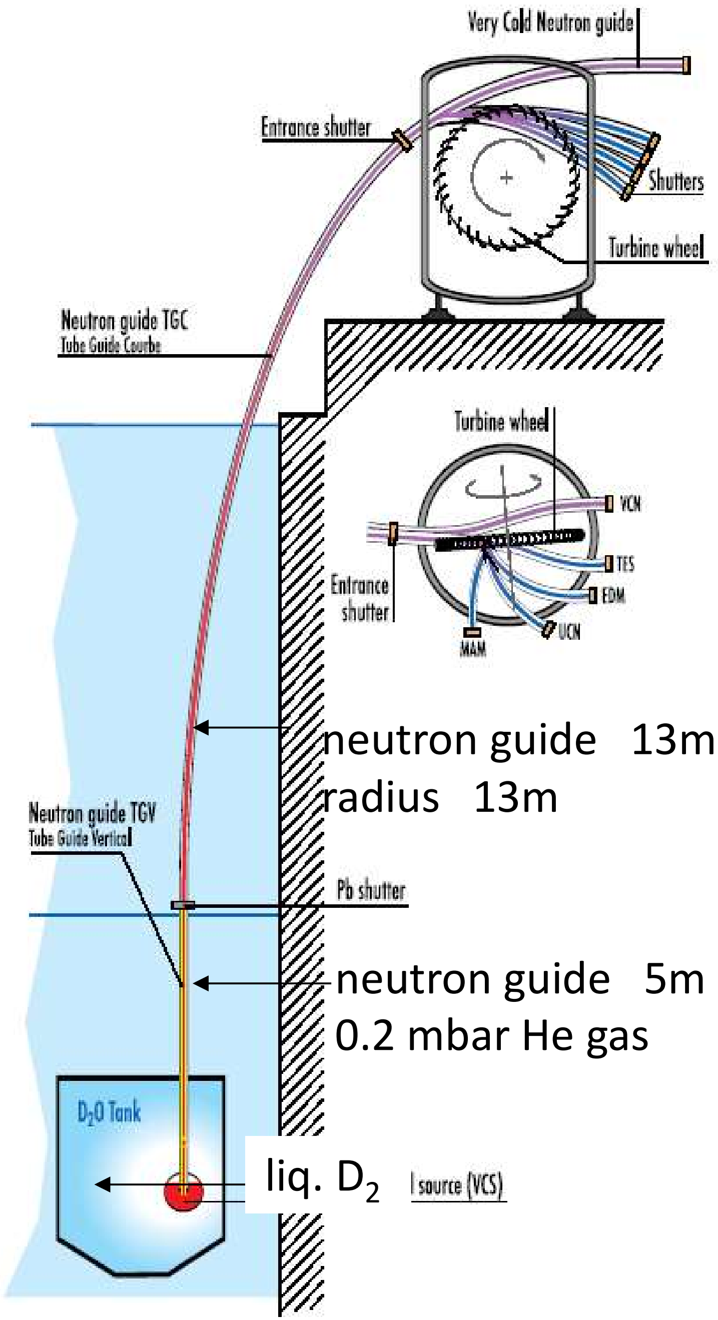

http://www.ill.fr/YellowBook/PF2

Super thermal method

- phonon down-scattering in super-fluid He or solid D_2
- use large phase space of phonon
- free from Liouville's theorem

We use superfluid helium as a UCN converter

neutron

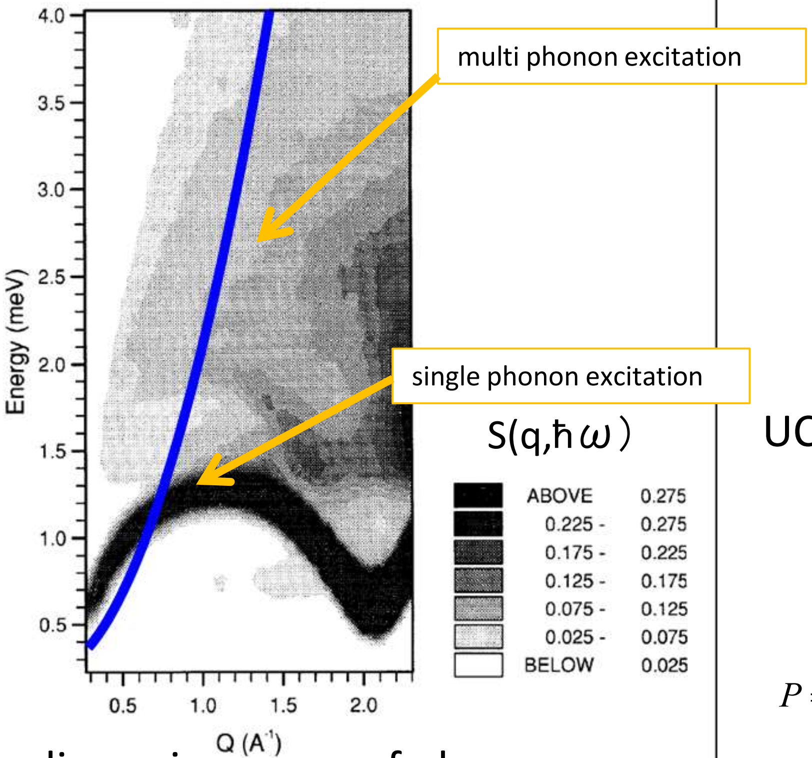

dispersion curve of phonon

M. R. Gibbs, et al
J. Low Temp. Phys. 120 (2000) 55

UCN production cross section

$$\frac{d\sigma}{dE} = 4\pi b^2 \frac{k_f}{k_i} S(q,\hbar\omega)$$

k_i, k_f : wavenumber

$S(q,\hbar\omega)$: Dynamic structure factor

resonant energy (single phonon excitation)

1 meV

UCN Production rate

$$P(E_u)dE_u = \left[\int \frac{d\Phi(E_i)}{dE} N_{\mathrm{He}} \frac{d\sigma}{dE}(E_i \to E_u) dE_i\right] dE_u$$

$$P = \int p(E_u)dE_u = N_{\mathrm{He}} 4\pi b^2 \left(\frac{\hbar}{m_n}\right)^2 \frac{k_c^3}{3} \left[\int \frac{d\Phi(q)}{dE} S\left(q, \hbar\omega = \frac{\hbar^2 q^2}{2m_n}\right) dq\right]$$

UCN production by super fluid Helium

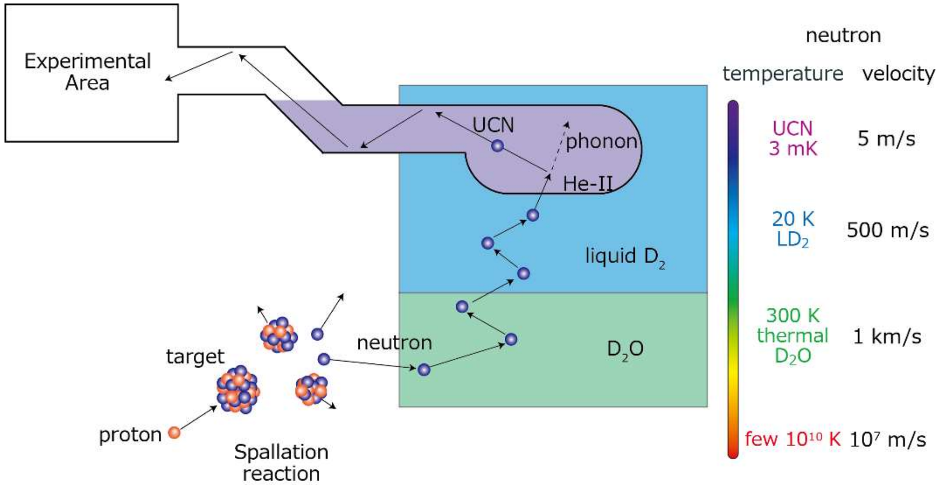

UCN production

spallation neutron ～ MeV

↓ D_2O Moderator (300K, 20K)

cold neutron ～meV

↓ Phonon scattering in He-II

Ultra cold neutron ～100neV

Feature

- spallation neutron
  - High neutron flux
    - small distance between target and HeII
  - High radiation Heat
- Super-fluid Helium converter
  - long storage lifetime
    - up-scattering by phonon
      - τ_s = 36 s at T_{HeII} = 1.2 K
      - τ_s = 600 s at T_{HeII} = 0.8 K
      - (Cf. SD_2 : T_s = 24ms)

T_{HeII} ～ 1.0 K is necessary

High intensity UCN source at PSI

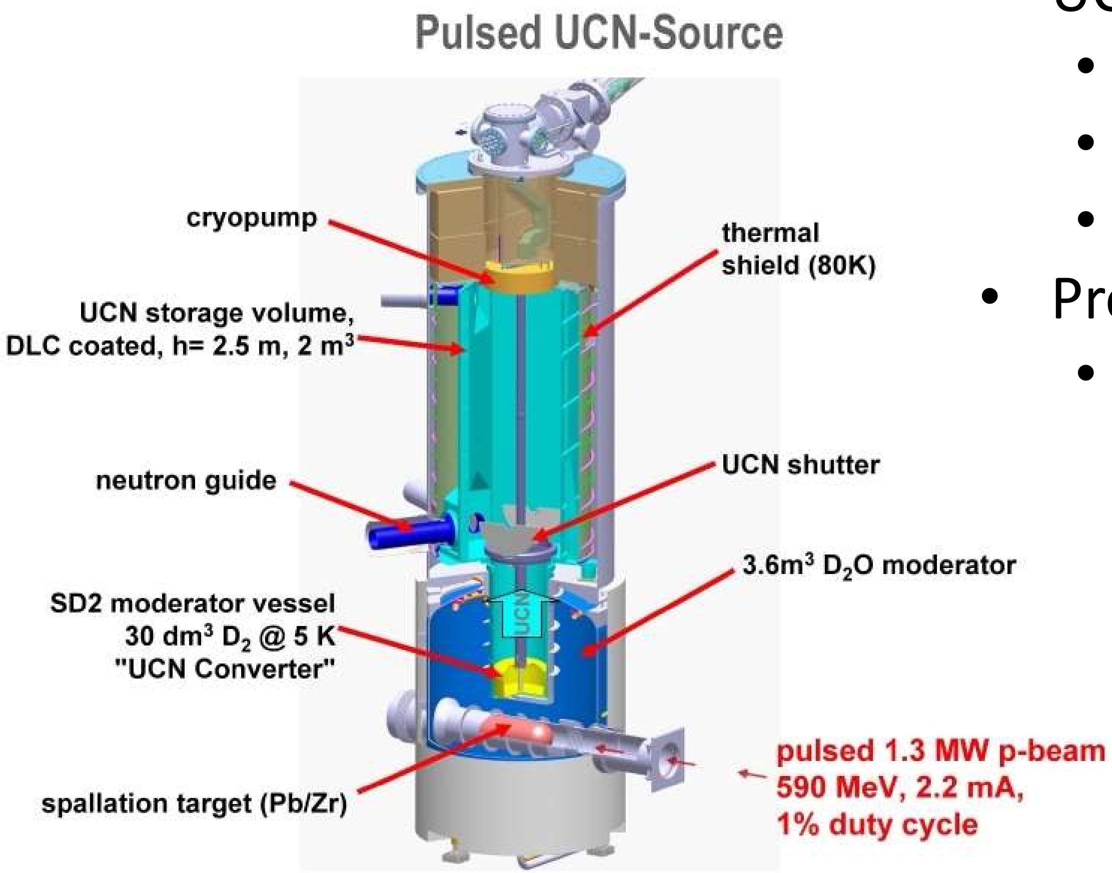

- UCN Converter
  - Solid Deuterium (SD_2)
  - Mass: 5 kg
  - Temperature: 5 K
- Proton Beam
  - power: 1.3 MW
    - 590 MeV, 2.2 mA
    - Duty cycle: 1%

neutron EDM measurement

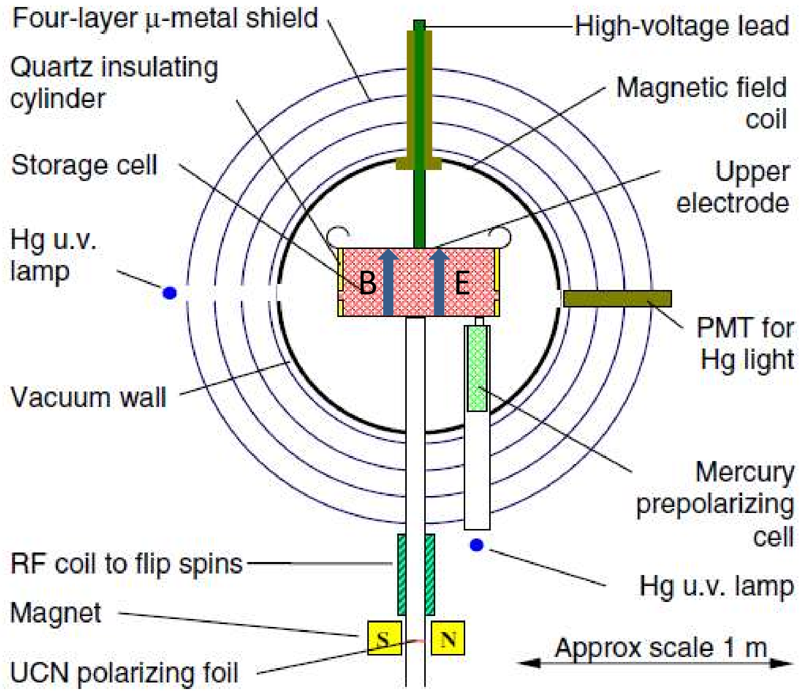

magnetic field	1μT
electric field	10kV/cm
t_c	130s

Phy. Rev. Lett. **97** .131801 (2006)

ラムゼー共鳴法

ある間隔をあけて粒子とコヒーレントな電磁場を2度相互作用させたときに生じる共鳴現象。時間間隔が大きい程共鳴の線幅は電磁場間の時間間隔に反比例して小さくなる

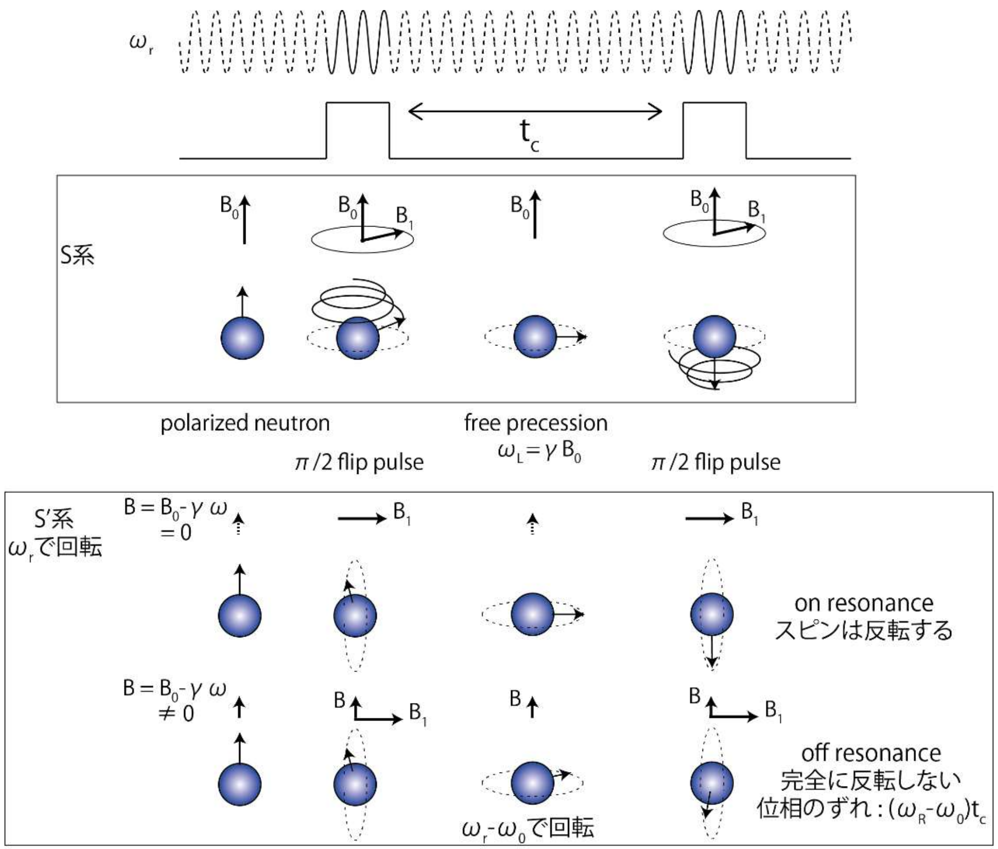

位相のずれがt_c間蓄積される

neutron EDM measurement

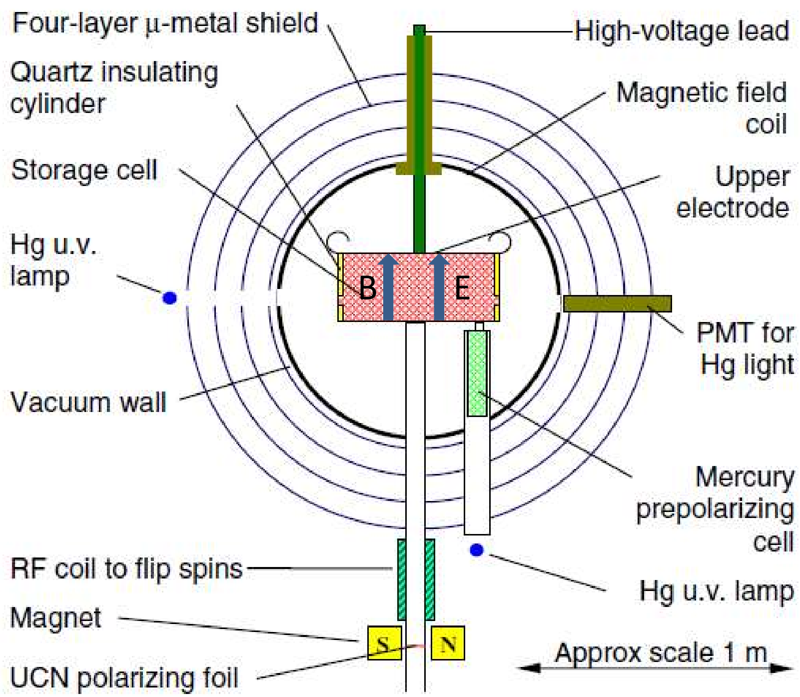

ラムゼー干渉縞

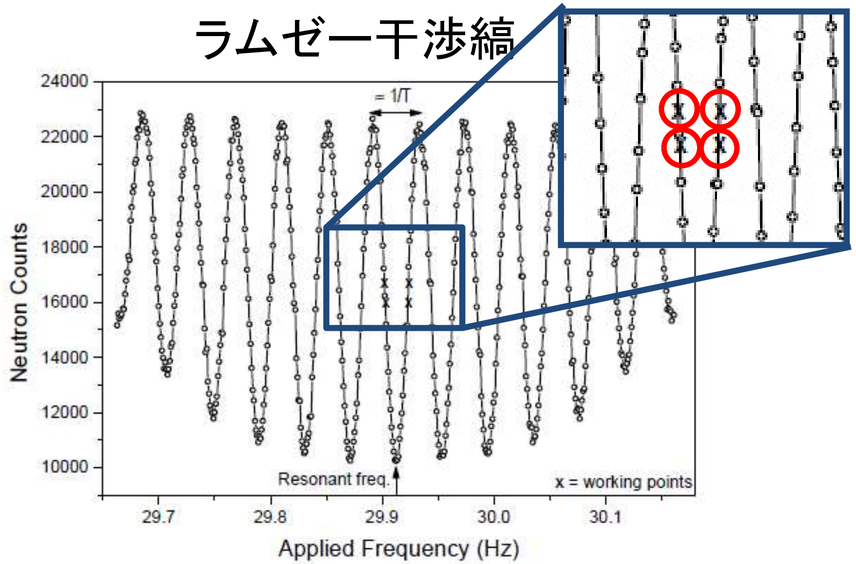

magnetic field	1μT
electric field	10kV/cm
t_c	130s

Phy. Rev. Lett. **97** .131801 (2006)

Statistical sensitivity

$$\boxed{\sigma_d = \frac{\hbar}{2\alpha E t_c \sqrt{N}}}$$

α : polarization (visibility)
E : electric field
t_c : precession time
N : number of UCN

co-magnetometer

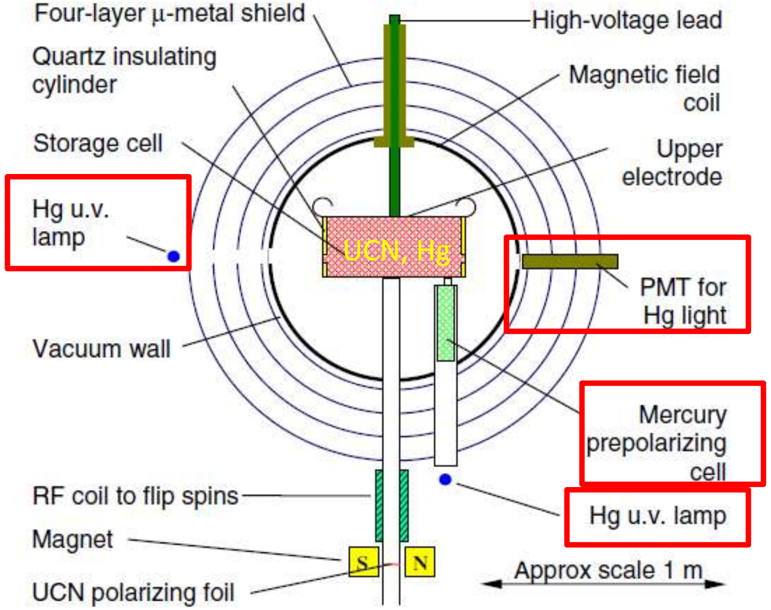

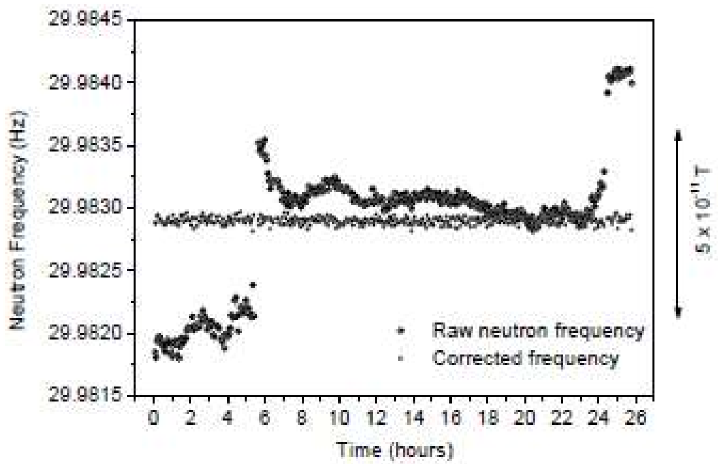

P. G. Harris *et al.*, Phys. Rev. Lett. **82**, 904 (1999).

frequency shift

$$\Delta\omega = 4 \times 10^{-7} Hz$$

(E = 10kV/cm, d = 10^{-27}ecm)

cf. Larmor frequency of neutron

30Hz @ B_0 = 1μT

required magnetic field stability : 10^8

1μT * 10^{-8} = 10 fT

It is difficult to stabilize magnetic field in such a accuracy

-> monitor and correct magnetic field

^{199}Hg for co-magnetometer

- feels same magnetic field as UCN
- polarization is measured by UV laser

Geometric Phase Effect

- Berry's phase
- 系統誤差の最大要因

Pendlebury et al, PRL 70, 032102 (2004)

- 水平方向磁場による周波数シフト(Bloch-Siegert shift)

$$\Delta\omega = \frac{{\omega_{xy}}^2}{2(\omega_0 - \omega_r)}$$

ω_r: angular speed of B_{xy} rotation

- 水平方向磁場

$$B_{xy} = \frac{\partial \mathrm{B_z}}{\partial \mathrm{z}}\frac{R}{2} + \frac{E \times v}{c^2}$$

  - 第1項: 磁場非一様性
  - 第2項: 相対論的運動
  - UCNの載っている座標から見るとBxyは回転しているように見える
  - 右、左回りで第2項のみ符号を変える

$$\Delta\omega_{ave} = \frac{1}{2}\frac{\gamma B_z\left[\left(\gamma\frac{\partial B_z}{\partial z}\frac{R}{2}\right)^2 + \left(\frac{v_\phi E_z}{c^2}\right)^2\right] + \gamma^2\frac{\partial B_z}{\partial z}\frac{R}{2}\frac{v_\phi \boxed{E_z}}{c^2}}{(\gamma B_z)^2 - (v_\phi/R)^2}$$

- 偽EDM
  - 電場反転したときの周波数差

$$d_{false}^{GPE} \approx \frac{\hbar\gamma^2\frac{\partial B_z}{\partial z}{v_\phi}^2 R^2/_{c^2}}{(\gamma B_z)^2 - (v_\phi/R)^2}$$

$\frac{\partial B_z}{\partial z} = 1\ \mathrm{nT/m}$ correspond error of 10-26 ecm

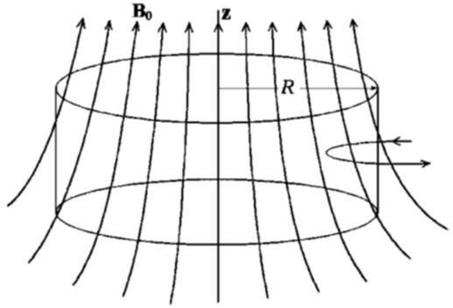

FIG. 1. (Color online) The shape of the $\mathbf{B}_0$ field lines, when there is a positive gradient $\partial B_{0z}/\partial z$, shown in relation to an outline of the trap used to store ^{199}Hg atoms and UCN's for the neutron EDM measurements at the ILL. If another field is superimposed having lines that both enter and leave through the sidewalls, like the one on the right-hand side, it will be shown later that it does not affect the false EDM signals that are generated.

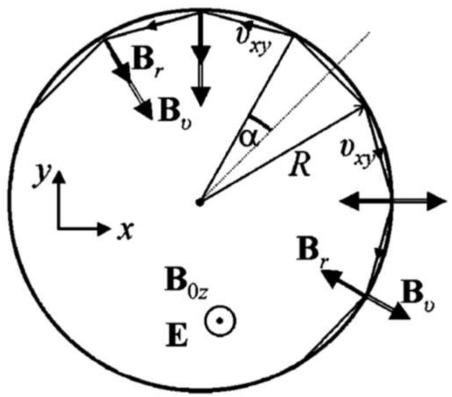

FIG. 3. (Color online) A view of the xy plane of the trap bounded by the circular sidewall. Part of an orbit is shown projected onto the xy plane for a particle undergoing specular reflection. The orbit is characterized by the angle α. Vectors $\mathbf{E}$ and $\mathbf{B}_{0z}$ point towards the reader and $\partial B_{0z}/\partial z$ is positive.

nEDM measurement at PSI

data accumulation

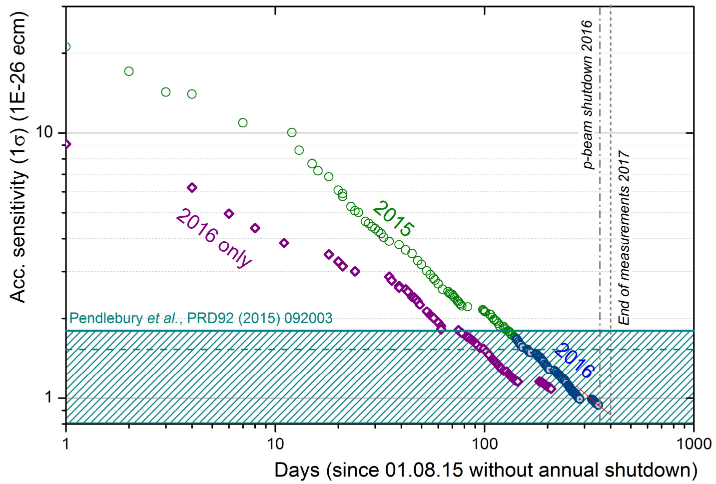

- Basically same setup as ILL experiment
  - Cell volume : 20 L
- 11400 UCN are counted per cycle
- data taken: 2015 – 2016
  up to reach 1×10^{-26} ecm statistical error
- Blind analysis by two grou

statistically limited

$$d_n = (0.0 \pm \underline{1.1_{stat}} \pm 0.2_{sys}) \times 10^{-26} \text{ ecm}$$
$$|d_n| < 1.8 \times 10^{-26} \text{ ecm (90\% C.L)}$$

C. Abel, et al, Phys. Rev. Lett. 124 81803 2020

Typical data cycle

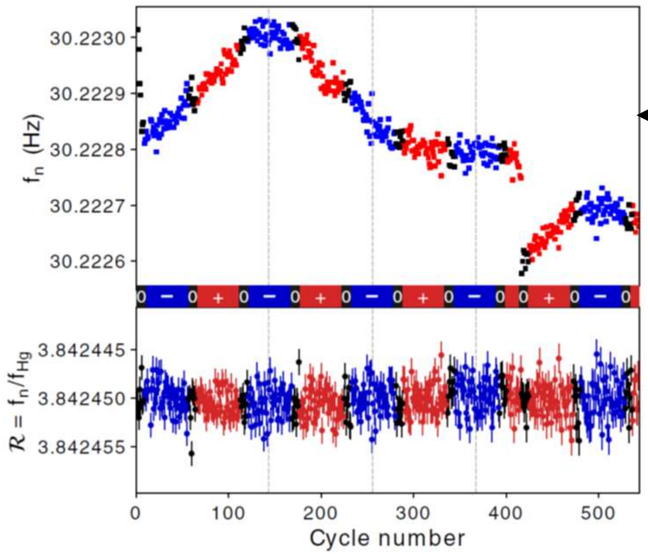

resonant frequency of neutron

E

correction by co-magnetometer

TABLE I. Summary of systematic effects in 10^{-28} e.cm. The first three effects are treated within the crossing-point fit and are included in $d_\times$. The additional effects below that are considered separately.

Effect	Shift	Error
Error on $\langle z \rangle$	...	7
Higher-order gradients $\hat{G}$	69	10
Transverse field correction $\langle B_T^2 \rangle$	0	5
Hg EDM [8]	−0.1	0.1
Local dipole fields	...	4
$v \times E$ UCN net motion	...	2
Quadratic $v \times E$	...	0.1
Uncompensated G drift	...	7.5
Mercury light shift	...	0.4
Inc. scattering ^{199}Hg	...	7
TOTAL	69	18

systematic error

PSI次期計画 n2EDM

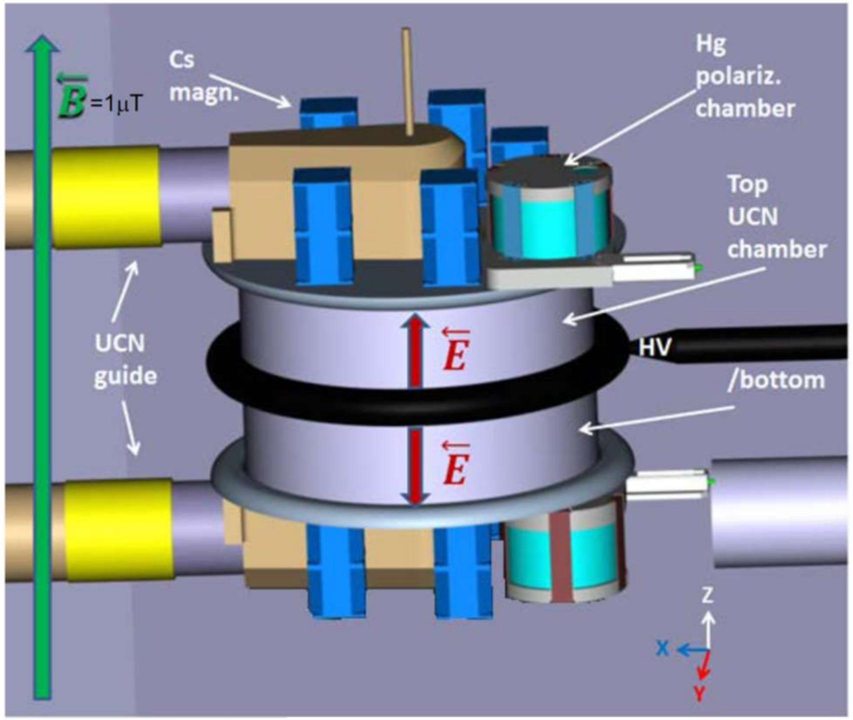

統計精度向上
- UCN密度は現行のまま
- 容器直径を大きく
  47 cm → 80 cm

系統誤差を抑えるのが課題
- 上下対称セルを用いて磁場ドリフトの影響をキャンセル
  - 同時に統計の増加にも寄与
- 磁気シールドルームを新設

B. Lauss, nEDM2017

	Current	n2EDM	n2EDM	n2EDM	n2EDM	n2EDM	n2EDM
phase	2016 average	comm.	comm.	meas.	meas.	meas.	meas.
ID (cm)	47	47	47	80	80	100	100
coating	dPS	dPS	iC	dPS	iC	dPS	iC
α	0.75	0.8	0.8	0.8	0.8	0.8	0.8
E (kV/cm)	11	15	15	15	15	15	15
T (s)	180	180	180	180	180	180	180
N	15′000	50′000	100′300	121′000	292′000	160′000	400′000
$\sigma(d_n)$ (e·cm) per day	11×10^{-26}	4.1×10^{-26}	2.8×10^{-26}	2.6×10^{-26}	1.7×10^{-26}	2.3×10^{-26}	1.4×10^{-26}
$\sigma(d_n)$ (e·cm) 500 data days	5.0×10^{-27}	1.8×10^{-27}	1.3×10^{-27}	1.2×10^{-27}	7.5×10^{-28}	1.0×10^{-27}	6.4×10^{-28}

TUCAN
(TRIUMF Ultra-Cold Advanced Neutron)

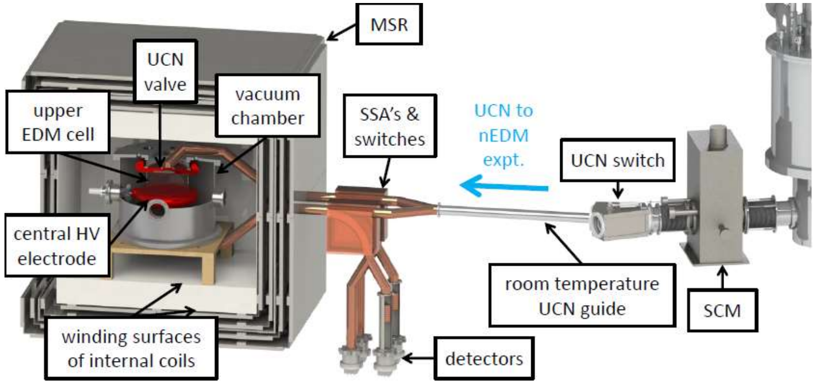

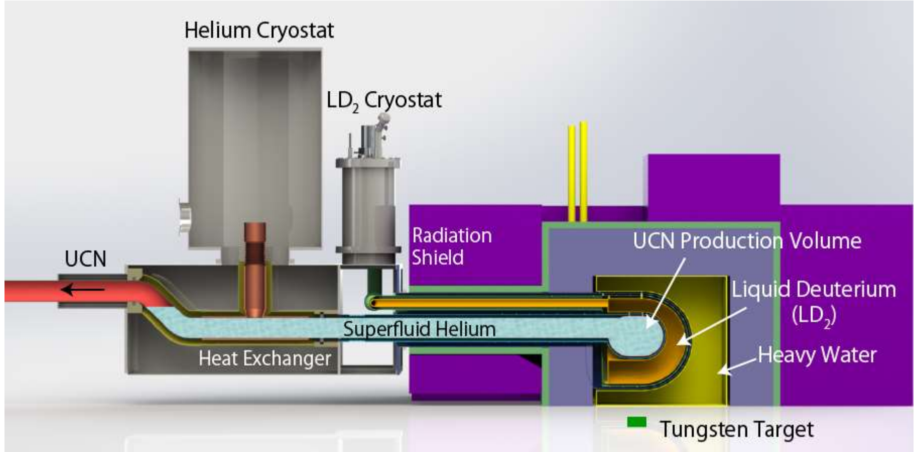

- 世界最大強度のUCN源を目指したアップグレード中
  - UCNコンバーター: 超流動ヘリウム
    - UCN loss: up scattering by phonon
    - これを抑えるためには超流動ヘリウム温度を1.0K以下に保たなければならない
    - 大型ヘリウム3冷凍機の開発
  - UCN源性能(設計値)
    - UCN密度
      - 6,400 UCN/cm^3 at production volume
      - 250 UCN/cm^3 at the EDM cells
  - KEKで大型ヘリウム3冷凍機製造、現在冷却テスト中
  - 2021年中にTRIUMFにインストール、2022年よりUCN生成予定
  - 400日のデータ取得により10^{-27} ecmの統計精度に達する見込み
- nEDM測定装置
  - 2023年よりのEDM測定を目指し、開発を進めている

Crystal EDM

- 結晶内を透過する冷中性子のスピン位相の変化を観測
- 結晶内の大きな有効電場を用いることによって感度をあげる
- 有効電場・体積の大きな結晶を用いるのが鍵

- Current best value

  dn = (2.5 ± 6.5stat ± 5.5sys) × 10^{-24} ecm at ILL

  V.V. Fedorov et al Phys. Lett. B 694, 22 – 25 (2010)
- 精度を上げげた実験がJ-PARCやESSで計画されている

E :strength of applied electric field

τ : interaction time

N : neutron counts

Sensitivity of nEDM experiment $\sigma(d_n) \propto \frac{1}{E\tau\sqrt{N}}$

	Free flight metod	Crystal diffraction method	UCN method
interaction tome τ [s]	～ 10^{-1}	～ 10^{-3}	～ 10^{2}
electric field E [V/cm]	～ 10^{4}	～ 10^{8}	～ 10^{4}
neutron counts n [n/s]	～ 10^{8}	～ 10^{4}	～ 10^{2}
sensitivity σ(d_n)	～$10^{-25}/\sqrt{\mathrm{Day}}$	～$10^{-25}/\sqrt{\mathrm{Day}}$	～$10^{-25}/\sqrt{\mathrm{Day}}$

パルス中性子源を用いた結晶回折によるnEDM探索

伊藤さん(名古屋大)のスライド

$$\varphi_{EDM} = \frac{2Ed_n L}{\hbar v_{//}}$$

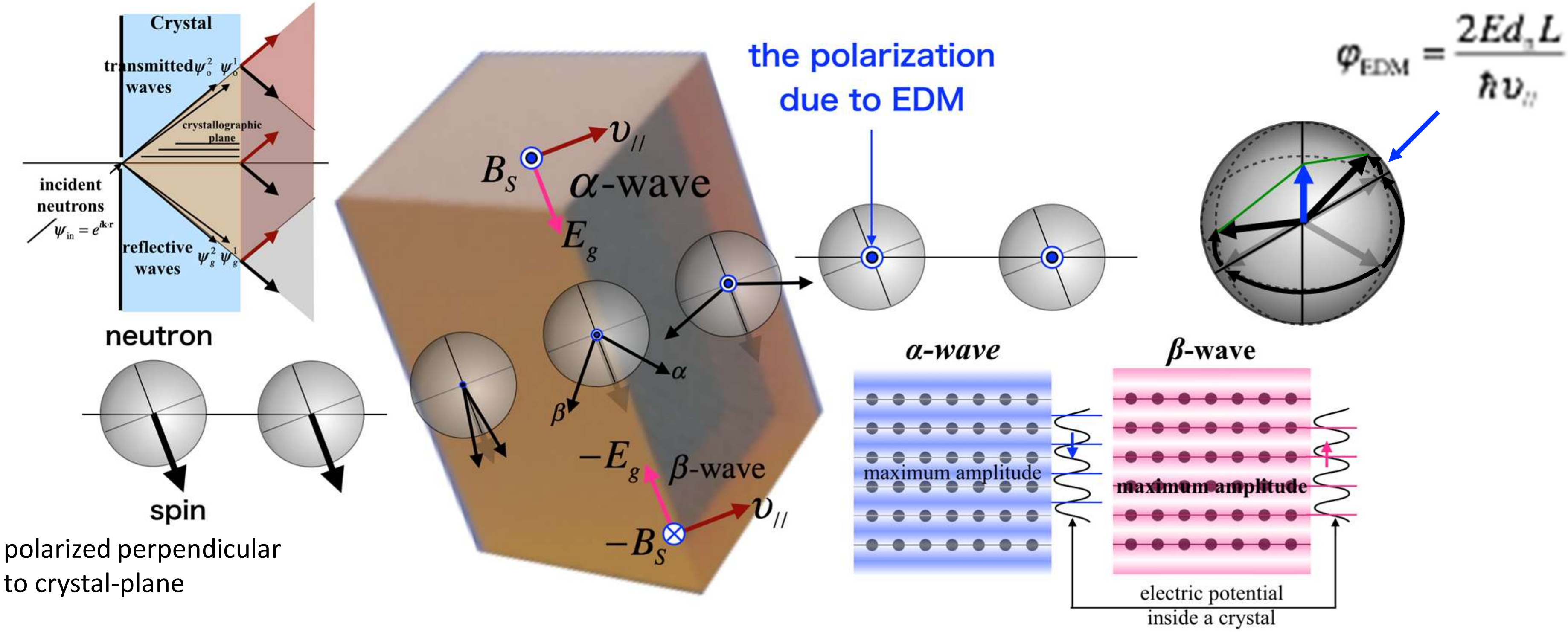

ペンデル縞を用いた結晶内電場の測定

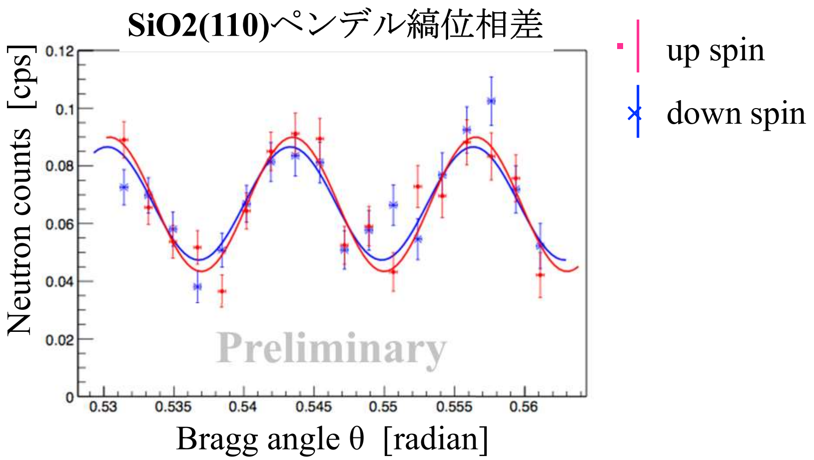

$$E_g = (0.40 \pm 1.47) \times 10^8 \ [\mathrm{V/cm}]$$

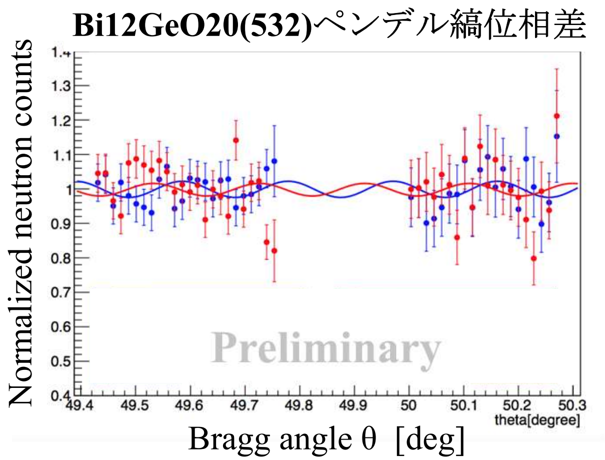

$$E_g = (3.5 \pm 2.0) \times 10^8 \ [\mathrm{V/cm}]$$

電子EDM

電子EDM

- 電場によって加速されてしまうため、荷電粒子のEDMを直接測定することは困難 (storage ring experimentを除く)

- 中性の粒子である、原子・分子のEDMを測定し、内部の荷電粒子のEDMを計算する
  - アルカリ金属(不対電子1)の場合
    - 電子は相対論的に振る舞う -> Shiffの定理は成り立たない
    - Cs, Tl, Fr
    - 相対論的効果による増幅機構

$$\propto Z^3$$

Tl: 585倍、Fr: 895 (最大)

- 分子
  - YbF, HfF^+, ThO
  - 大きな有効磁場
    - ThO E ＝78 GV/cm

Electron EDM: Tl

- Tl原子
  - 増幅率 585
- 測定step
  - Tl原子をレーザー(378 nm)によって偏光
  - RF照射 (1/2π)
  - 電極間を飛行
    - 電位 123 kV/cm
    - 2つの独立した経路(電場は逆向き)
  - RF照射 (1/2πにわずかな位相差)
  - レーザーを照射し、その蛍光を検出することにより共鳴周波数を求める
- Na: Co-magnetometer

$$|d_e| < 1.6 \times 10^{-27}\ \mathrm{ecm}$$

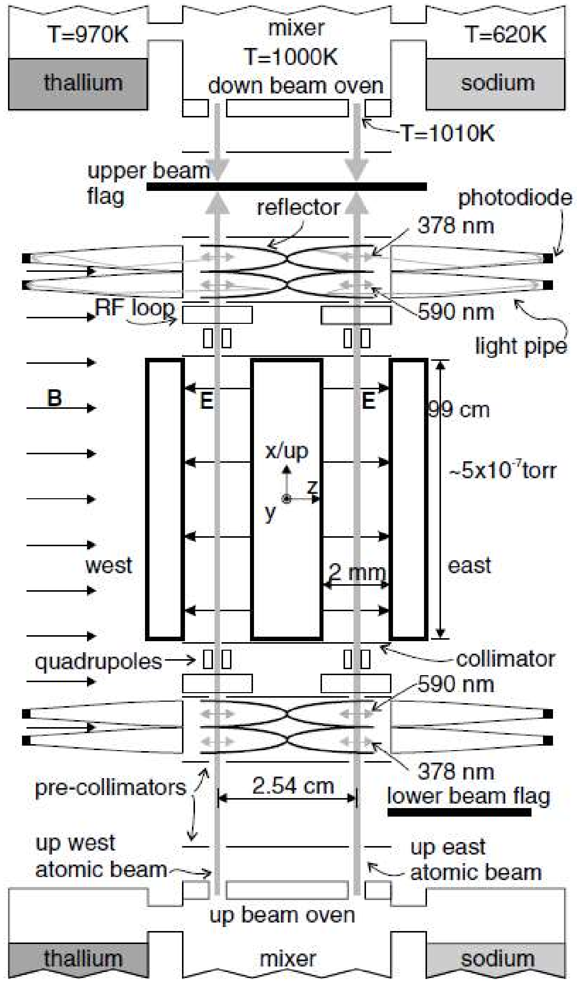

B.C. Regan et al,
PRL 88, 071805 (2002)

フランシウム　東大・理研・東北大

EDM with cooled/trapped atom

Francium（^{210}Fr）

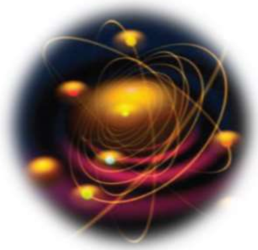

- Heaviest Alkali element
- $T_{1/2}$～3 min. : enough for online exp.
- Laser cooling/trapping : possible
- EDM enhancement : largest ～895

Relativistic coupled cluster model calculation
Phys.Rev.A93 (2016) 032520

×

Optical lattice

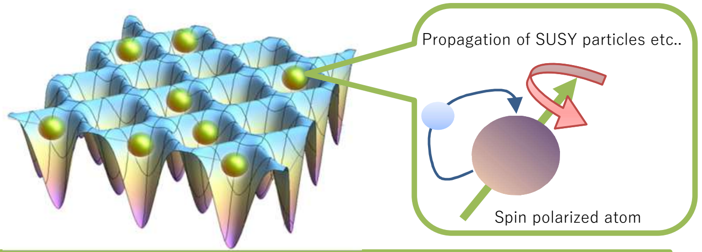

- Cold atom（~uK）
- Interaction between atoms ～ weak
- High vacuum ～ high electric field
- Long coherence time ～ sec. order

$$\delta d = \frac{\hbar}{2e} \cdot \frac{1}{K} \cdot \frac{1}{E} \cdot \frac{1}{\sqrt{N \cdot \tau \cdot T}}$$

Enhancement factor | Electric field | Trapped number | Coherence time: Long

Accuracy : $\dfrac{895(Fr)}{114(Cs)} \times \sqrt{\dfrac{1(trap)}{10^{-3}(beam)}} > 100$ **Times improved**

Slide by Y. Sakemi

Experimental setup

Nuclear fusion reaction : ^{18}O (~100 MeV) + ^{197}Au → $^{215-x}Fr$ + xn

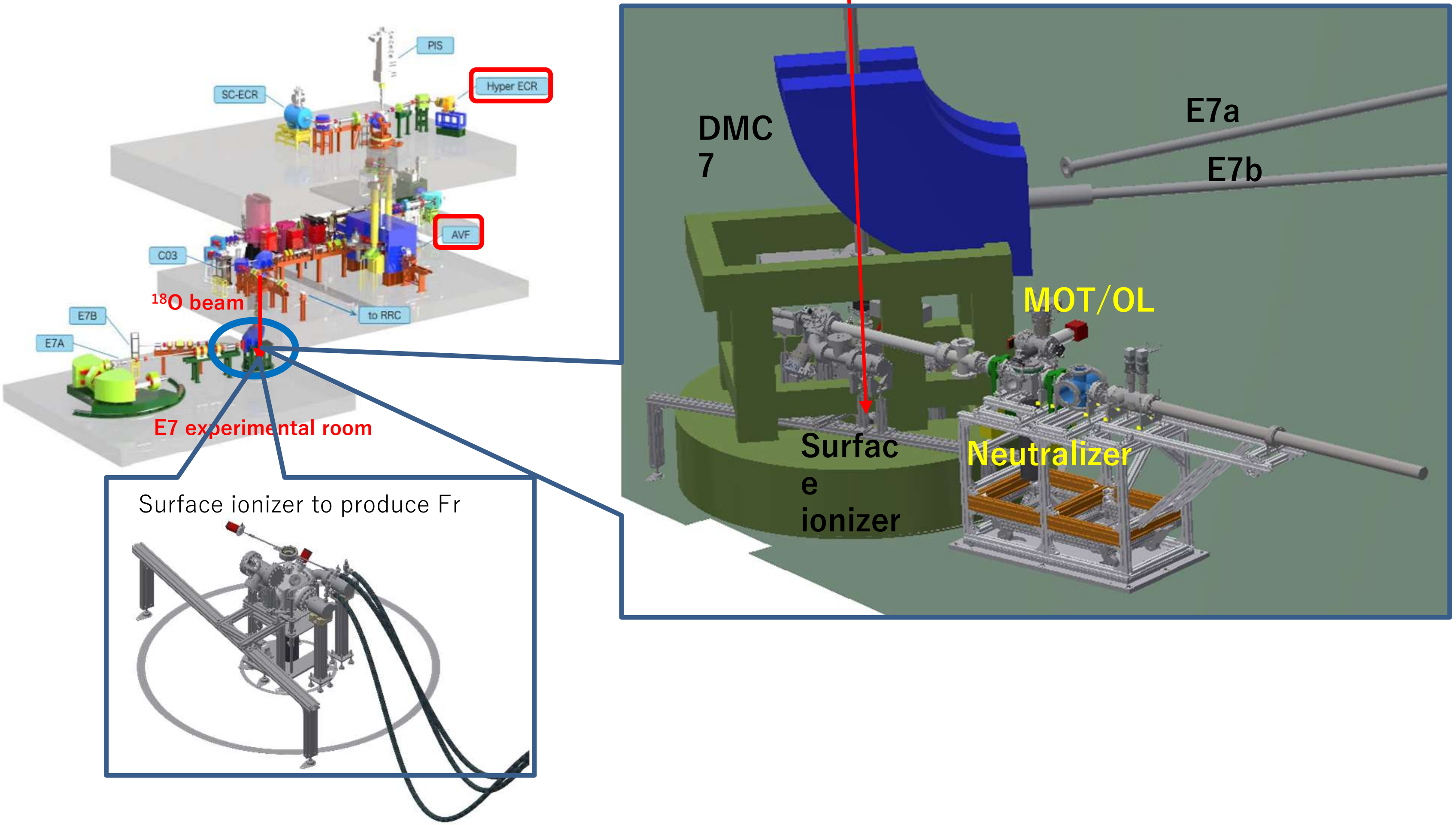

Slide by Y. Sakemi

Present status

- High intensity Fr source ~ successfully developed and operated at RIKEN
- Cold Fr source with MOT (Magneto-Optical Trap) ~ technique established
- Dual atoms co-magnetometer ~ demonstrated and established

- Fr yield: ~ 10^7 Fr^+/s
- Extraction efficiency : 10% - 20% achieved

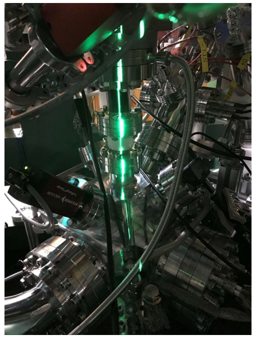

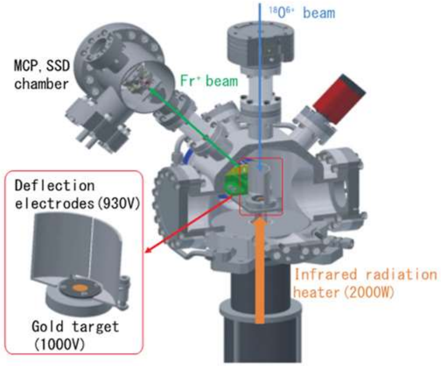

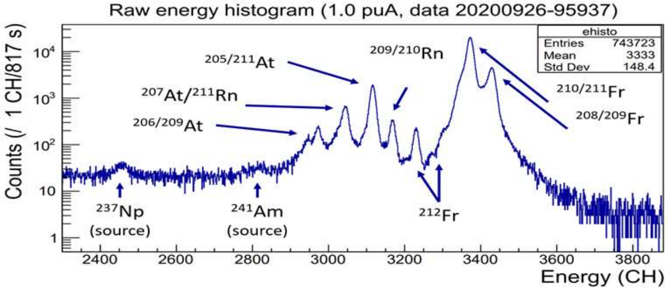

Laser cooled Fr source ~ stable supply (Appl. Opt. 55 (2016) 1164)

- Laser frequency stabilization with iodine molecules
- Offset locking of trapping and repumping laser

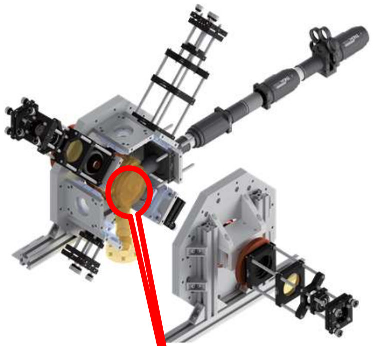

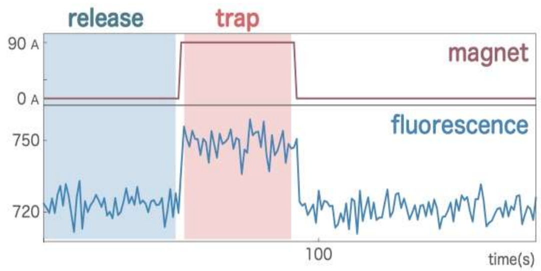

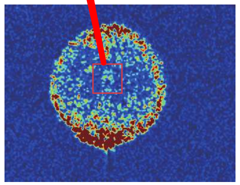

MOT ON

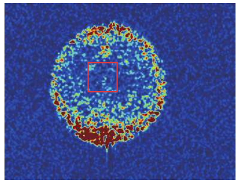

MOT OFF

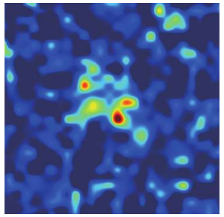

Slide by Y. Sakemi

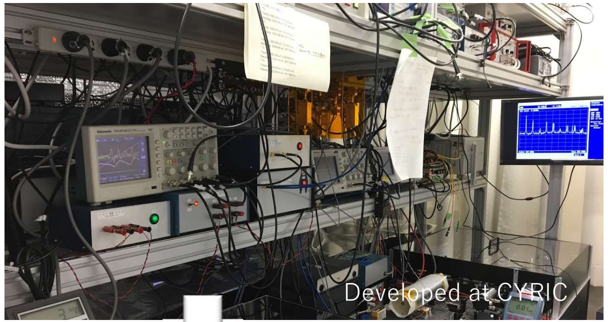

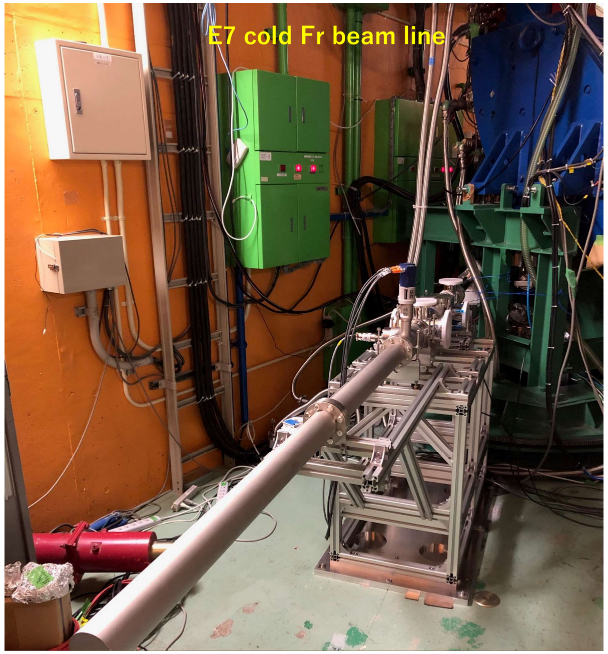

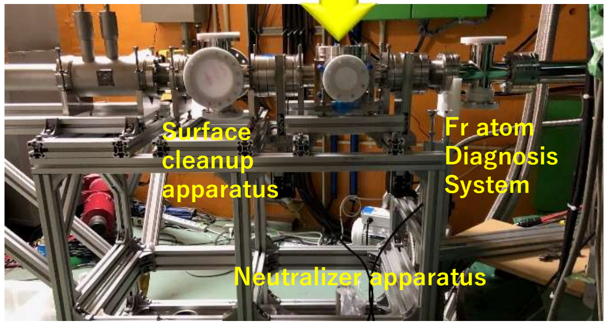

Slide by Y. Sakemi

分子EDM ThO

電子EDM

2010年以降、**極性分子**を用いたEDM測定が実現.
分子内部の大きな有効電場を用いることで、
測定感度が大きく向上している.

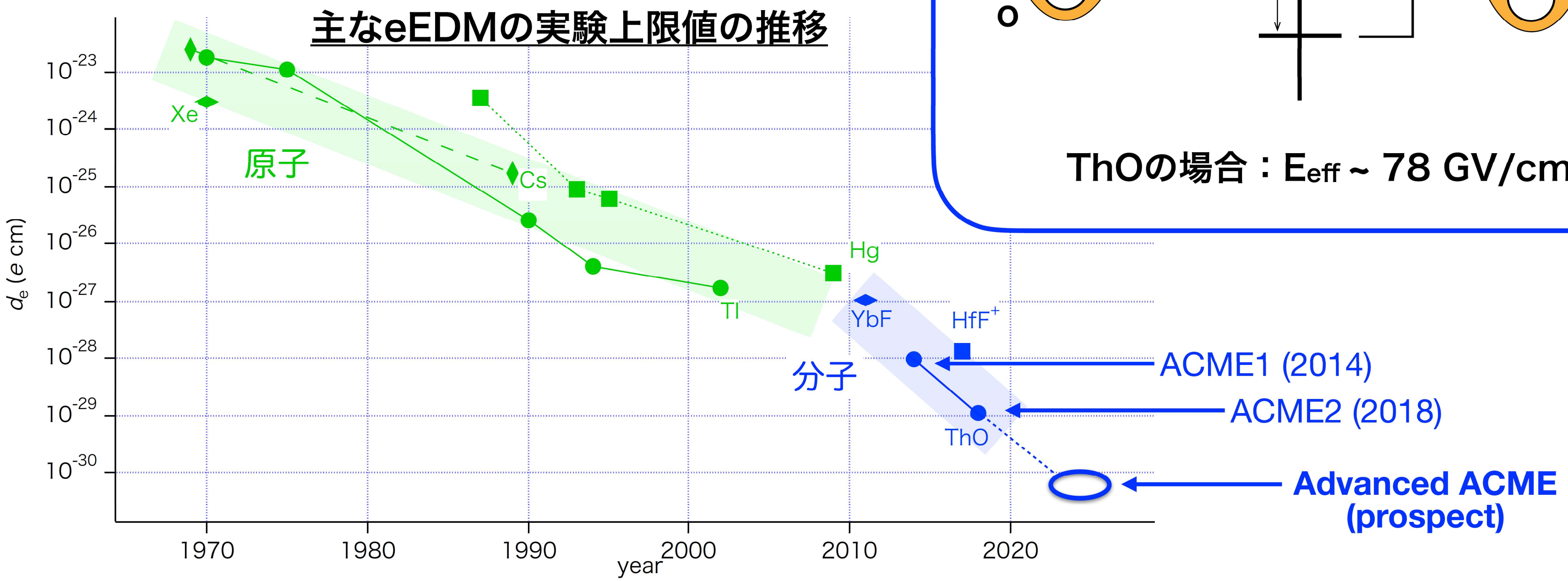

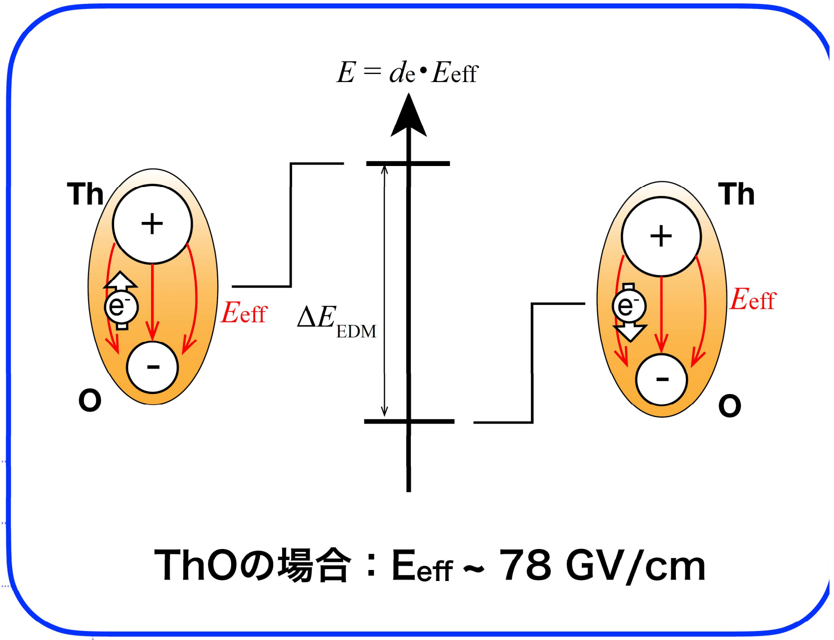

slide by 増田さん(岡山大)

Advanced ACME : |d_e| 測定感度30倍を目指して、アップグレード中

① 分子レンズを導入し
有効分子数 ~20倍

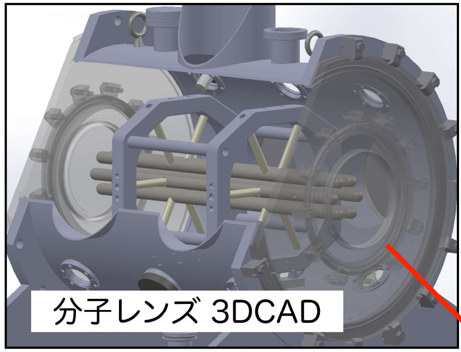

③ 蛍光検出部の
高感度大面積化
有効光子数 ~3倍

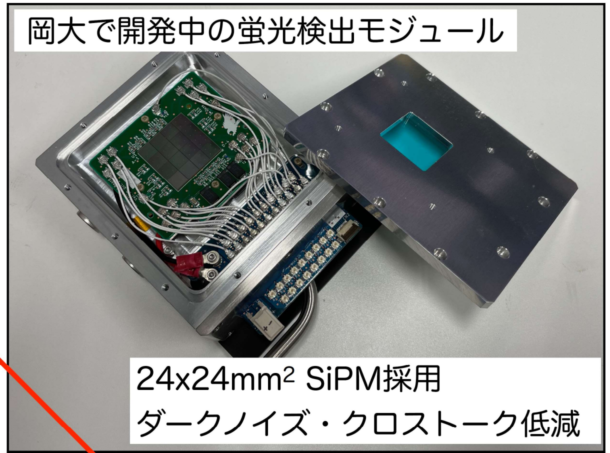

② 相互作用領域を延長し
スピン歳差時間を5倍延長

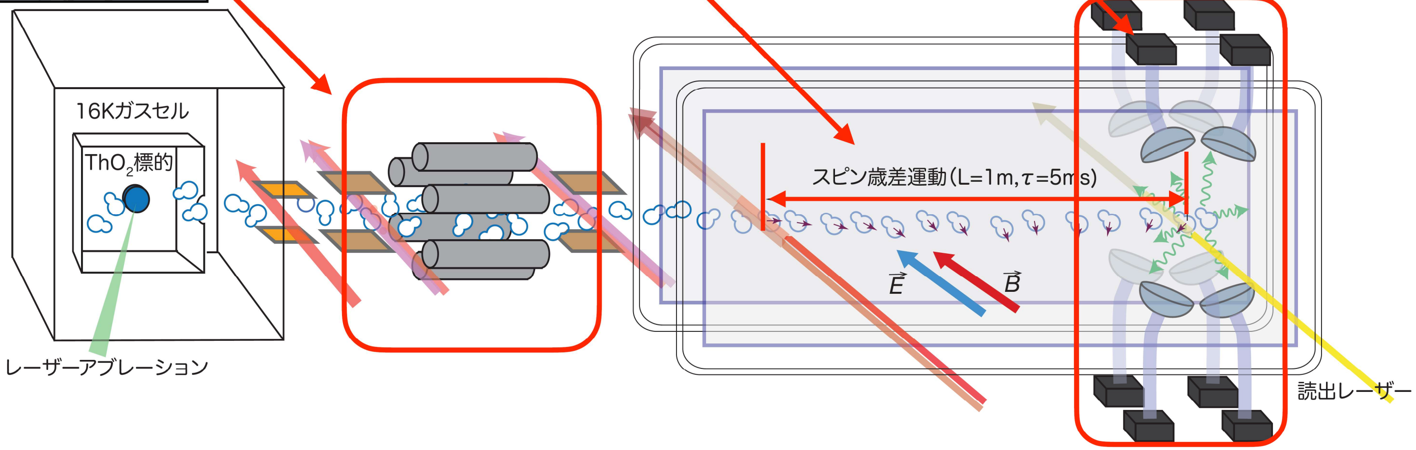

その他、磁気シールドや標的、DAQ、レーザーシステム、回転式レーザー窓などのアップグレードが進行、計画中

slide by 増田さん(岡山大)

Atomic EDM

- 反磁性原子 (閉殻構造)
  - Xe, Hg
- 常温でガス状(蒸気)であり、長いコヒーレンス時間を持つため、検出効率が上がりやすい
  - $d_{Hg} < 7.4 \times 10^{-30}$ ecm すべてのEDM実験で最小値
- オプティカルポンピングによる偏極

^{199}Hg

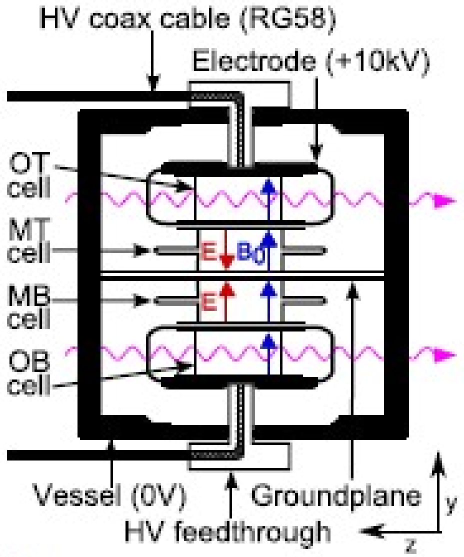

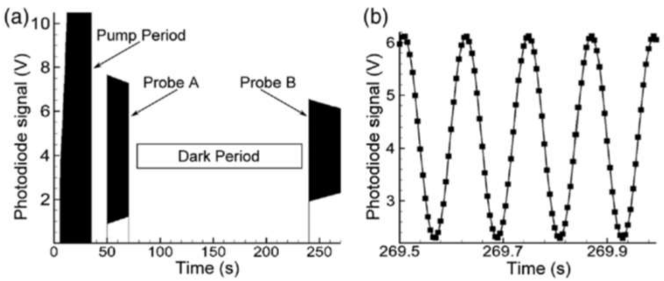

FIG. 2. The signal obtained from a single photodiode for one pump-probe cycle. (a) A complete view of the signal. During optical pumping, the transmission through the cell increases, quickly saturating the detector. The laser power is reduced during the probe periods *A* and *B*, which are analyzed to extract the phase difference accumulated between cells during the dark period. Individual Larmor oscillations are too rapid to be visible at this scale, but the exponential decay of the signal envelope can be seen. (b) An expanded view of the final 500 ms of the data train. The raw data points are connected by straight line segments to guide the eye; no fit is shown.

B.Graner, PhysRevLett.116.161601 (2016)

Four vapor cells
Φ 25mm, H 10.1 mm
Hg ~ 0.5 mg
$C0_2$: 0.56 atm　buffer gas

pump/probe by UV lazer

4つのセルを用いる
outer cells: magnetometer
inner cells : E field opposite

測定サイクル
- 光ポンピング
- 周波数測定
- Free precession (dark period)
- 周波数測定

プローブ光による減偏極を避ける

$|d_{Hg}| < 7.4\times 10^{-30}$ ecm
これまで測られたEDMの最小値

^{129}Xe

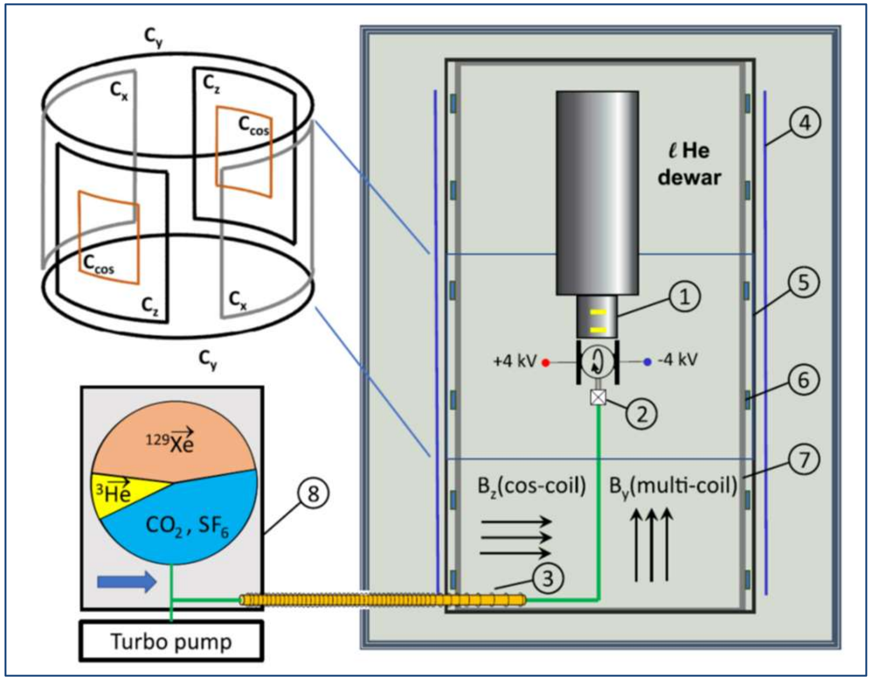

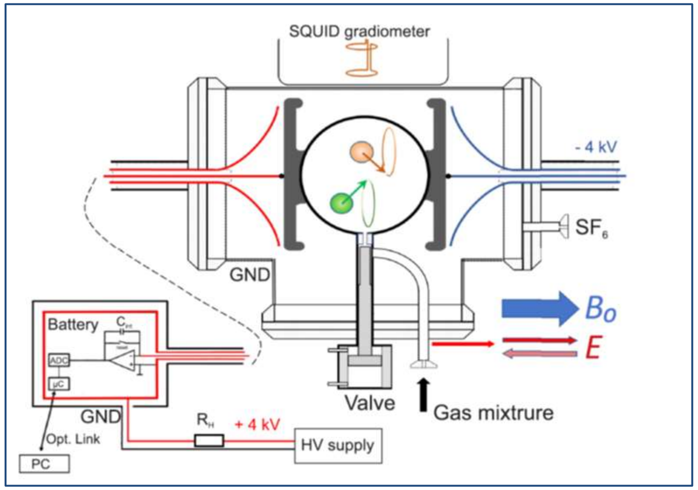

F. Allmendinger et al, Pnys. Rev. A, 100, 2505m, (2019)

- ^{3}He/^{129}Xe混合ガス
  - ^{3}He : comagnetometer
- SQUID:　スピン歳差運動検出

長いスピン緩和時間

- ^{129}Xe: 3,700 – 8,000 sec
- ^{3}He:　4,000 – 8,000 sec

高性能の磁気シールド

磁場非一様性 50 – 300 pT/cm

d_{Xe} = (-4.7 ± 6.4) × 10^{-28} ecm

upper limit

d_{Xe} < 1.5 × 10^{-27} ecm

F. Allmendinger et al, Phys. Rev. A 100, 022505 (2019)

再解析

d_{Xe} < 8.3 × 10^{-28} ecm

T. Liu *et al*., *arXiv* 2008.07975 (2020)

Summary

- 有限の値のEDMの存在 → T対称性の破れ
  (CPT対称を仮定すれば) CP対称性の破れ
- 様々な系でEDMの測定がされているが、いまだに有限の値は見つかっていない
- 現行(&近未来)の実験感度は標準理論の計算するEDMに届かないので、観測されれば、新物理法則による
- その新物理の性質を明らかにするには様々な系でのEDM観測が重要

Schiff's theorem

- Charged constitutes are significantly shielded from the large external field by the polarization of the atom
- For bound system of point like charged particles the net force and the net electric field at the position of each charged particle are exactly zero.
- The shielding is not perfect for a nucleus of finite size and in the case of unpaired electron (paramagnetic system) due to relativistic effects.

Schiff's Theorem

for a nonrelativistic system made up of point, charged particles which interact electrostatically with each other and with an arbitrary external field, the shielding is complete

- Diamagnetic atom : Hg, Xe, Rn, Ra...
  - Schiff's screening argument is violated by finite-size effects.
- Paramagnetic atom : Tl, Fr, Cs....
  - Schiff's screening argument is violated by relativistic effects.

EDM measurement

- Measure precession frequency under electro-magnetic field

$$H = -\vec{\mu}\cdot\vec{B} + \vec{d}\cdot\vec{E}$$

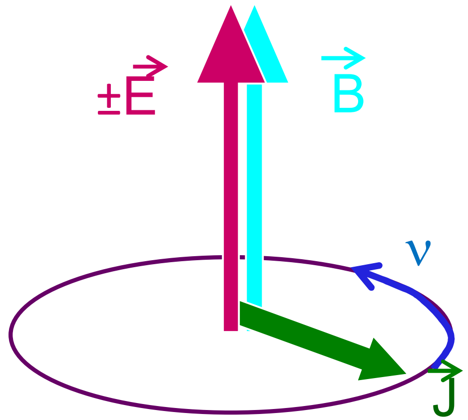

$$\hbar\omega = 2\mu_n B \pm 2d_n E$$

precession frequency

$$\hbar\omega = 2\mu_n B \pm 2d_n E$$

difference

$$\Delta\omega = \omega_{\uparrow\uparrow} - \omega_{\uparrow\downarrow} = \frac{4dE}{\hbar}$$

in case of dn = 10^{-27}ecm, E= 10 kV/m

$$\Delta\omega = 4 \times 10^{-7} Hz$$

cf. Larmor frequency of neutron

30Hz @ B_0 = 1μT

GPE

Pendlebury et al. *PRA* **70**, 032102 (2004)

False nEDM due to GPE under the magnetic field B_{0z} with the field gradient $\partial B_{0z}/\partial z$

$$\boxed{d_{fn} = -\frac{\hbar}{6}\frac{\langle v_n^2\rangle}{c^2}\frac{1}{{B_{0z}}^2}\frac{\partial B_{0z}}{\partial z}}$$

(adiabatic)

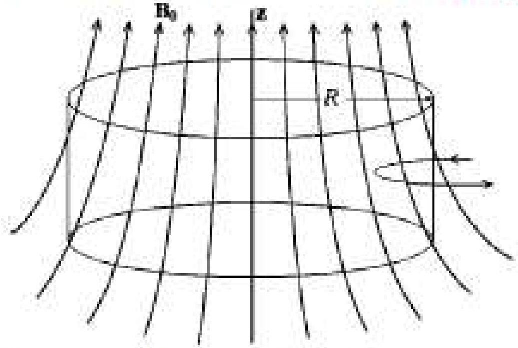

Precession frequency of polarized Hg $\omega_{\mathrm{Hg}\uparrow\uparrow}$

$$\omega_{\mathrm{Hg}\uparrow\uparrow} = -\gamma_{\mathrm{Hg}} B_{0z}$$

with the field gradient $\partial B_{0z}/\partial z$ and the electric field E (non-adiabatic)

$$\omega_{\mathrm{Hg}\uparrow\uparrow} = -\gamma_{\mathrm{Hg}} B_{0z} - \frac{\gamma_{\mathrm{Hg}}^2 R_{\mathrm{Hg}}^2}{2c^2}\frac{\partial B_{0z}}{\partial z}E + \frac{\gamma_{\mathrm{Hg}}^3 R_{\mathrm{Hg}}^2}{2c^4} B_{0z} E^2 + \frac{3\gamma_{\mathrm{Hg}}^3 R_{\mathrm{Hg}}^4}{16\langle v_{\mathrm{Hg}}^2\rangle} B_{0z}\left(\frac{\partial B_{0z}}{\partial z}\right)^2$$

Precession frequency of polarized Xe $\omega_{\mathrm{Xe}\uparrow\uparrow}$

$$\omega_{\mathrm{Xe}\uparrow\uparrow} = -\gamma_{\mathrm{Xe}} B_{0z} - \frac{\gamma_{\mathrm{Xe}}^2 R_{\mathrm{Xe}}^2}{2c^2}\frac{\partial B_{0z}}{\partial z}E + \frac{\gamma_{\mathrm{Xe}}^3 R_{\mathrm{Xe}}^2}{2c^4} B_{0z} E^2 + \frac{3\gamma_{\mathrm{Xe}}^3 R_{\mathrm{Xe}}^4}{16\langle v_{\mathrm{Xe}}^2\rangle} B_{0z}\left(\frac{\partial B_{0z}}{\partial z}\right)^2$$

Slide by T. Momose

GPE

Pendlebury et al. *PRA* **70**, 032102 (2004)

False nEDM due to GPE under the magnetic field B_{0z} with the field gradient $\partial B_{0z}/\partial z$

$$\boxed{d_{fn} = -\frac{\hbar}{6}\frac{\langle v_n^2\rangle}{c^2}\frac{1}{{B_{0z}}^2}\frac{\partial B_{0z}}{\partial z}}$$

(adiabatic)

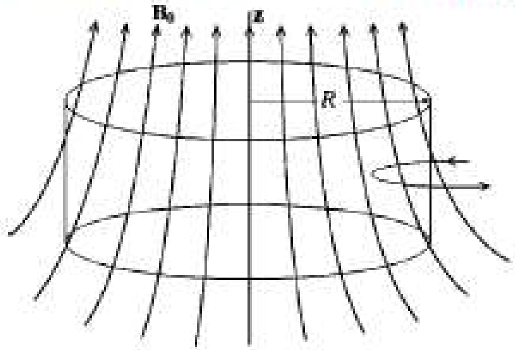

Precession frequency of polarized Hg $\omega_{\mathrm{Hg}\uparrow\uparrow}$

$$\omega_{\mathrm{Hg}\uparrow\uparrow} = -\gamma_{\mathrm{Hg}} B_{0z}$$

with the field gradient $\partial B_{0z}/\partial z$ and the electric field E

(non-adiabatic)

$$\boxed{\omega_{\mathrm{Hg}\uparrow\uparrow} = -\gamma_{\mathrm{Hg}} B_{0z} - \frac{\gamma_{\mathrm{Hg}}^2 R_{\mathrm{Hg}}^2}{2c^2}\frac{\partial B_{0z}}{\partial z}E + \frac{\gamma_{\mathrm{Hg}}^3 R_{\mathrm{Hg}}^2}{2c^4}B_{0z}E^2} + \frac{3\gamma_{\mathrm{Hg}}^3 R_{\mathrm{Hg}}^4}{16\langle v_{\mathrm{Hg}}^2\rangle}B_{0z}\left(\frac{\partial B_{0z}}{\partial z}\right)^2$$

Precession frequency of polarized Xe $\omega_{\mathrm{Xe}\uparrow\uparrow}$

$$\boxed{\omega_{\mathrm{Xe}\uparrow\uparrow} = -\gamma_{\mathrm{Xe}} B_{0z} - \frac{\gamma_{\mathrm{Xe}}^2 R_{\mathrm{Xe}}^2}{2c^2}\frac{\partial B_{0z}}{\partial z}E + \frac{\gamma_{\mathrm{Xe}}^3 R_{\mathrm{Xe}}^2}{2c^4}B_{0z}E^2} + \frac{3\gamma_{\mathrm{Xe}}^3 R_{\mathrm{Xe}}^4}{16\langle v_{\mathrm{Xe}}^2\rangle}B_{0z}\left(\frac{\partial B_{0z}}{\partial z}\right)^2$$

Hence for each fill, these two equations can be solved for **the two unknowns**

B_{0z} and $\dfrac{\partial B_{0z}}{\partial z}$

Slide by T. Momose